Int J Adv Manuf Technol (2017) 88:2305–2320
DOI 10.1007/s00170-016-8952-2

ORIGINAL ARTICLE

Energy consumption modeling of machining transient states based on finite state machine

Shun Jia[1] · **Renzhong Tang**[2] · **Jingxiang Lv**[3] · **Qinghe Yuan**[1] · **Tao Peng**[2]

Received: 11 January 2016 / Accepted: 18 May 2016 / Published online: 31 May 2016

Abstract Energy-saving and emission reduction are urgently vital tasks of the manufacturing industry. Energy optimization of machining processes provides an important approach leading to the energy-saving of the manufacturing industry. Energy modeling of machining processes is the key technology and foundation of energy optimization. Energy consumption of machining processes can be decomposed into two parts: energy consumption of steady state and energy consumption of transient state. Transient state is the transition process between two steady states, which may lead to the peak power. Transient states frequently occur during a machining process and their energy consumptions should not be ignored. However, research that specifically focuses on these energies is rare. Therefore, a finite state machine (FSM)-based energy consumption modeling method of machining transient state is proposed in this paper. FSM is introduced to describe the transient states during machining. The key transient state processes are identified according to Pareto principle, and energy consumption models of these key transient state processes are established. State transition chart is then constructed to determine key transient states and their execution times during machining process. Based on the state transition chart and energy consumption models of the key transient states, an energy consumption model of machining process is established. Finally, a case study is conducted to show the effectiveness and feasibility of the proposed modeling method. The proposed method can improve the integrity and accuracy of the energy consumption model of machining process.

Keywords Transient state · Energy consumption modeling · Finite state machine (FSM) · State transition chart · Sustainable machining

✉ Shun Jia
herojiashun@163.com

✉ Renzhong Tang
tangrz@zju.edu.cn

[1] Shandong University of Science and Technology, Qingdao 266590, China

[2] Industrial Engineering Center, Zhejiang Province Key Laboratory of Advanced Manufacturing Technology, Zhejiang University, Hangzhou 310027, China

[3] Key Laboratory of Contemporary Design and Integrated Manufacturing Technology, Ministry of Education, Northwestern Polytechnical University, Xi'an 710072, Shaanxi, China

1 Introduction

Due to growing energy price and increasing environmental pollution, significant energy and resource consumption in the manufacturing industry has received increasing attention in recent years [1]. Energy consumption is one of the most significant factors that lead manufacturing enterprises to become environmentally unfriendly [2]. It has been shown that nearly one third of the world's energy consumption and 36 % of CO_2 emissions are attributable to manufacturing industries [3]. In China, manufacturing industry consumes around 50 % of the entire electricity produced [4] and generates at least 26 % of the total CO_2 emissions. It is obvious that the manufacturing industry has become one of the major sources of energy consumption and carbon emissions. Therefore, energy-saving and emission reduction is an urgently vital task of the manufacturing industry. Machining process, as a major process of manufacturing industries [5], plays an important role in energy-saving and emission reduction. An interesting research conducted by Gutowski [6] showed that CO_2 emission by a computer numerical control (CNC) machine tool

(22 kW spindle power) in 1 year is equivalent to 61 SUVs' CO_2 emissions driving a year (20.7 mpg, 12,000 mi). Additionally, a life cycle analysis (LCA) of a machine tool conducted by Zulaika et al. [7] showed that 95 % of environmental impact of machine tools is associated to use phase (10-year lifespan) and from that use phase impact, 95 % comes from energy consumption.

As mentioned above, energy consumption and carbon emission of machining process are very huge. Triggered by the necessity to improve the energy efficiency and environmental performance of machining processes, energy modeling and saving of machining processes has received increasing attention [8–19]. Actually, energy consumption of machining process can be divided into two categories: energy consumption of steady state and energy consumption of transient state [20]. Transient state is the transition process between two machining activities, which may lead to frequent peak power during a machining process [21–24], as shown in Fig. 1. Energy consumptions of machining transient states should not be ignored if an accurate energy consumption prediction of machining process is desired. However, research that especially focuses on energy consumption of machining transient state is rare. To fill this gap, a finite state machine (FSM)-based energy consumption modeling method of machining transient state is proposed in this paper.

2 Literature review

Although energy modeling and energy efficiency improvement issues of machining processes have been discussed in some existing literatures [25–27], attentions paid on energy consumption of machining transient state are not enough. Machining transient state generally relates to motor starting, instant increment of momentum or torque of moving parts, etc. Thus, it will cause the peak power phenomena and such phenomena have been reflected in many studies [28–32]. However, further research and analysis of the reason and energy consumption characteristic of peak power are not given in the abovementioned references. Although the duration of transient state process is short, the caused peak power is significant [28, 33] and transient state processes frequently appear in machining process, leading to the significant energy consumption during machining process. The energy consumption of transient states (spindle startup) is usually neglected or regarded as a part of the no-load energy. These treatments may result in significant errors under certain machining conditions [34, 35]. Balogun et al. [31] indicated that the power spikes occur during machine startup (transient state), and these spikes need clarification and adequate modeling. The calculated energy value is 9.3 % smaller than the measured value in the case study of literature [36], one important reason is that the energy consumption of transient states was not taken into account. It is visible that energy consumption of transient state is an important part of energy requirements during machining process. However, research that specially focuses on the energy consumption of machining transient state is rare.

Reinhart et al. [37] proposed a comparison method of resource efficiency (materials, energy) for different process chains. Although a peak power phenomenon of spindle startup was measured, the energy consumption of spindle startup process was directly neglected and further research about energy consumption of spindle startup was not mentioned. Avram and Xirouchakis [38] researched the energy consumed during the use of machine tools, and the acceleration and deceleration power models of spindle and feed axis were established based on the torque and angular velocity. However, some parameters (friction torque and torque required for overcoming the spindle rotary inertia) in the model are very difficult to obtain, which makes the model difficult to apply in practice. The energy consumption of spindle startup process is viewed as a single value, and the energy consumption of spindle accelerating from static state to different speeds was measured. Quadratic function was used to describe the energy consumption of spindle startup process [39]. The model can be applied to calculate energy consumption of spindle accelerating from static state to a specified rotation speed. When the initial state of spindle is not static, due to the various initial speed, it is not realistic to measure the energy consumptions from any initial speed to a specified rotation speed. In

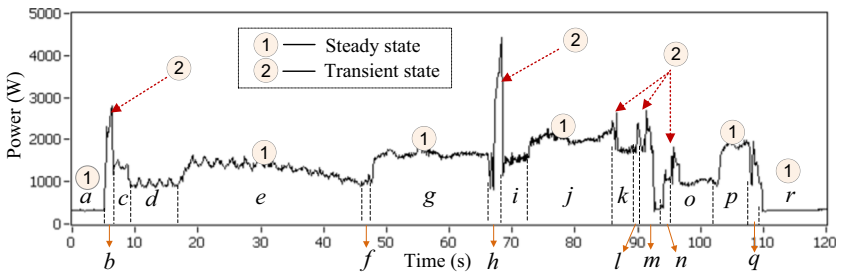

Fig. 1 Measured power curve of machining process for a shaft part. **a** standby operating; **b** spindle speedup to 500r/min; **c** rapid positioning; **d** feeding; **e** end-face turning; **f** rapid positioning+feeding; **g** rough turning; **h** rapid positioning+Spindle speedup to 1000r/min; **i** feeding; **j** finish turning; **k** Rapid positioning+feeding; **l** Chamfering; **m** Rapid positioning+Spindle speed to 500r/min; **n** Tool changing; **o** Rapid positioning+feeding; **p** grooving; **q** rapid positioning to origin; **r** standby operating,machining finised

addition, the power change during spindle startup process cannot be reflected and the peak power of acceleration process cannot be calculated with the above model. Similarly, Huang et al. [35] proposed an approach to determine the spindle startup energy consumption before machining and the startup process is defined as the spindle accelerates from zero to its target speed n_s, when the auxiliary systems are all in steady states. Therefore, when the spindle accelerates from a lower speed (not zero) to a higher speed during machining, the above approach could not be applied as well. Lv [40] established the energy supply model of spindle acceleration by using theoretical modeling and experimental analysis. The model can calculate the energy consumption of spindle system during spindle speedup process. However, in addition to the motion of spindle system, machine standby operating, feeding, coolant spraying, chip conveying, and other motions are possible to be executed during spindle acceleration process. Hence, the actual energy consumption of the spindle speedup process is the sum of the energy consumption of above motions. Whether these motions are executed or not are dynamic and it is dependent on the machining state during spindle speedup. Therefore, only in determining the machining states during the spindle acceleration can we accurately calculate the total energy consumption of the spindle speedup process.

As mentioned above, although the duration of transient state process is short, the caused peak power is large; energy consumption of transient state process should not be ignored if an accurate energy prediction of machining process is desired. The references mentioned above mostly refer to the peak power phenomenon caused by the transient state, but quantitative analysis and energy consumption models of transient states are not further studied. Energy consumption of spindle startup was researched in several preliminary literatures; however, the types of transient state processes are varied, including spindle startup, fast positioning acceleration, coolant start, tool change start, and so on. Energy consumptions characteristic of different transient states are various and related to the machining states during the transient state process. Up to now, there is still a lack of an energy consumption model of machining transient state, which can systematically consider the difference of energy consumption characteristics of different types of transient states. It can be seen that the energy consumption modeling of machining transient state should be further studied. Machining process consists of a series of steady states and transient states. Transient state is the transition process between two steady states, which corresponds to the machining state transition of CNC machine tools. Finite state machine (FSM) could exactly describe finite number of states and the transition behaviors among these states [41, 42]. Therefore, FSM is introduced to describe the finite number of machining states and transitions among machining states. A FSM-based energy consumption modeling method of machining transient state is proposed in this paper.

3 Modeling methodology

3.1 Description of transient state-based on FSM

3.1.1 Finite state machine

FSM is composed of finite number of states and state transitions. The machine is in only one state at a time; it can change from one state to another when initiated by a triggering event or condition and simultaneously generate an output [41–43]. A typical FSM can be expressed by a five-tuple [42].

$$M = \left(Q, \sum, \Delta, \sigma, q_0\right) \tag{1}$$

where Q is state set, $Q = \{q_0, q_1, \cdots, q_m\}$; $\sum$ is input event set, $\sum = \{\sum_0, \sum_1, \cdots, \sum_n\}$; Δ is output event set, $\Delta = \{\Delta_0, \Delta_1, \cdots, \Delta_l\}$; σ is transition function mapping $Q \times \sum$ to $Q \times \Delta$; q_0 is initial state, $q_0 \in Q$.

FSM can also be demonstrated with a state transition chart [42], as shown in Fig. 2. Each elliptic node represents a state and the arc without a source state points to the initial state, i.e., state α. Each arc represents a transition and each transition is labeled by "I/O," where $I \in \sum$ represents an input event that triggers the transition, and $O \in \Delta$ represents an output event when the transition is triggered. Taking the basic state transition chart in Fig. 2 as an example, state set is $Q = \{\alpha, \beta\}$; input set is $\sum = \{a, b, c\}$; output set is $\Delta = \{m, n, \varepsilon\}$; state transitions are $\sigma(\alpha, a) = (\beta, m)$, $\sigma(\beta, b) = (\alpha, n)$ and self-transition $\sigma(\beta, c) = (\beta, \varepsilon)$; initial state is $q_0 = \alpha$.

3.1.2 Description of transient state with FSM

Machining process can be decomposed into a series of activities and each activity only in one machining state at a time [44, 45]. Transient state process corresponds to the transition process between two machining states. Figure 3 shows the state transition chart from state i to state j (corresponding to transient state from state i to j) where elliptic node represents machining state and arc represents state transition. $\sum_k$ labeled on the left side of "/" represents input event that triggers the transition; $\Delta_{i,j}$ labeled on the right side of "/" represents output information when the transition is triggered. $\Delta_{i,j}$ consists of two

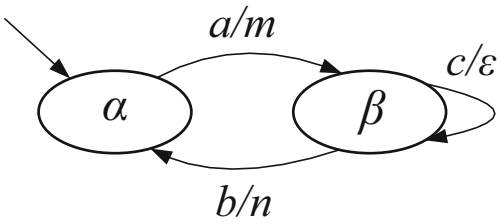

Fig. 2 A basic state transition chart of FSM

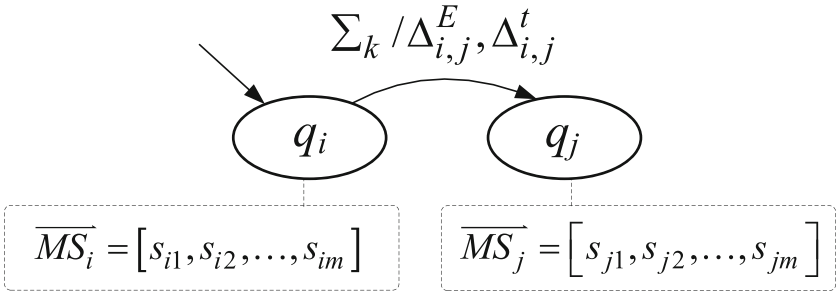

Fig. 3 State transition chart of state i to state j

parts: $\Delta_{i,j}^E$ (energy consumption of state transition from i to j)) and $\Delta_{i,j}{}^t$ ((duration of state transition from i to j). $\overrightarrow{MS_i}$ and $\overrightarrow{MS_j}$ are state vectors of state i and state j, respectively. s_{im} is logistic representation of executing state of therblig m during state i; s_{jm} is logistic representation of executing state of therblig m during state j. s_{im} and s_{jm} are 0–1 variables. The state transition in Fig. 3 can be expressed as $\sigma(q_i, \sum_k) = (q_j, \Delta_{i,j})$.

A therblig of CNC machine tool is defined as a basic motion and is also a basic energy consumption unit of a CNC machine tool. Fourteen types of therbligs of CNC machine tools are defined from an energy perspective. For detailed information about therbligs of CNC machine tools, you can refer to reference [20, 44]. Generally, operations of commonly used CNC machine tools are composed of 11 types of therbligs. Hence, state vector $\overrightarrow{MS}$ is composed of logistic representations of executing states of 11 types of therbligs ($m = 11$): $\overrightarrow{MS} = [s_1, s_2, \cdots, s_{11}]$, as shown in Fig. 4. $s_1 \sim s_{11}$ is a logistic representation of executing state of therblig-standby operating Ⓢ, lighting ⊗, cutting flood spraying ≋, chip conveying ⊔, spindle rotating ◯, X-axis feeding Ⓧ, Y-axis feeding Ⓨ, Z-axis feeding Ⓩ, tool selecting, tool changing, and material cutting Ⓒ, respectively. When therblig is executed then the corresponding $s = 1$; otherwise, $s = 0$.

Take machining state "q_1 standby" and "q_2 spindle idling" as an example, state transition $q_1 \rightarrow q_2$ is shown in Fig. 5. Machining state q_1 standby changes to state q_2 spindle idling when triggered by an input event "$\sum_8$." Consequently, the corresponding state vector changes from $\overrightarrow{MS_1} = [1, 1, 0, 0, 0, 0, 0, 0, 0, 0, 0]$ to $\overrightarrow{MS_2} = [1, 1, 0, 0, 1, 0, 0, 0, 0, 0, 0]$. Energy consumption and duration of the above state transition is expressed by $\Delta_{1,2}{}^E$ and $\Delta_{1,2}{}^t$, respectively. The state transition in Fig. 5 is expressed as $\sigma(q_1, \sum_8) = (q_2, \Delta_{1,2})$.

3.1.3 Classification of transient states

As mentioned above, state vector is composed of logistic representations of executing states of 11 types of therbligs. Supposing state vectors of state i and state j are $\overrightarrow{MS_i} = [s_{i1}, s_{i2}, \ldots, s_{i11}]$ and $\overrightarrow{MS_j} = [s_{j1}, s_{j2}, \ldots, s_{j11}]$, respectively. Then, machining transient states are classified according to the state evolution of different types of therbligs, as shown in Table 1.

Energy consumption of each type of transient state in Table 1 is researched by means of experimental study, and the key transient states are figured out according to the Pareto principle. Taking machine tool CK6153i as an example, energy consumption of each transient state can be obtained by using the experimental setup built by our research group. More information about the experimental setup can be found in reference [45]. The energy consumptions of transient state "chip conveying (off → on)" and "lighting (off → on)" are estimated values for the reason that there is no automatic chip conveying device on the abovementioned machine tool, and the lighting device cannot be controlled separately. Transient states "lighting(on → off)/cooling(on → off)/chip conveying(on → off)/tool changing(on → off)/machine tool (on → off)" only involve instantaneous closing of the lighting device or motor. Consequently, energy consumptions of the above five transient states are all very small (given 5 J). The Pareto chart is obtained according to the energy consumption value of each transient state gained by experimental study, as shown in Fig. 6.

Based on the above Pareto chart and 80/20 rule, top 20 % of transient states (top four) ranked by energy consumptions are taken as key transient states. The transient state "machine tool (off → on)" can be divided into three sub-movements: start air switch, start NC control panel, and release emergency stop button. The above three sub-motions are manual operations

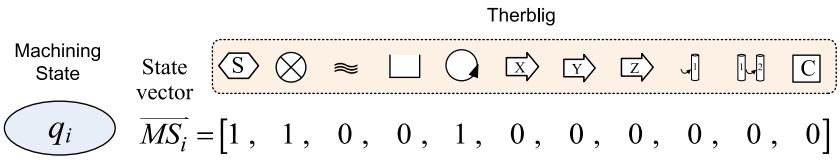

Fig. 4 Composition of state vector

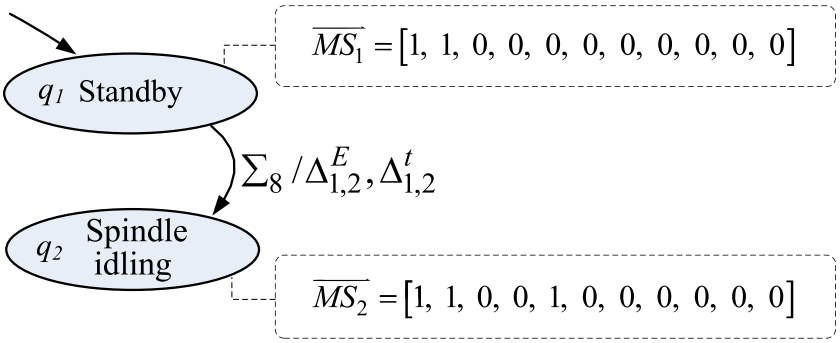

Fig. 5 Example of state transition

Table 1 Classification of transient states

Transient state	Condition	Corresponding transfer function
Machine tool (off → on)	$s_{i1} = 0$ and $s_{j1} = 1$	$\sigma(q_0, \sum_0) = (q_1, \Delta_{0,1})$;
Machine tool (on → off)	$s_{i1} = 1$ and $s_{j1} = 0$	$\sigma(q_1, \sum_1) = (q_0, \Delta_{1,0})$
Lighting (off → on)	$s_{i2} = 0$ and $s_{j2} = 1$	$\sigma(q_i, \sum_2) = (q_j, \Delta_{i,j}), i = j = 1,2,\ldots,10$
Lighting (on → off)	$s_{i2} = 1$ and $s_{j2} = 0$	$\sigma(q_i, \sum_3) = (q_j, \Delta_{i,j}), i = j = 1,2,\ldots,10$
Cooling(off → on)	$s_{i3} = 0$ and $s_{j3} = 1$	$\sigma(q_1, \sum_{11}) = (q_1, \Delta_{1,1})$; $\sigma(q_2, \sum_{11}) = (q_2, \Delta_{2,2})$; $\sigma(q_3, \sum_{11}) = (q_3, \Delta_{3,3})$; $\sigma(q_4, \sum_{11}) = (q_4, \Delta_{4,4})$; $\sigma(q_5, \sum_{11}) = (q_6, \Delta_{5,6})$; $\sigma(q_7, \sum_{11}) = (q_8, \Delta_{7,8})$
Cooling (on → off)	$s_{i3} = 1$ and $s_{j3} = 0$	$\sigma(q_1, \sum_{12}) = (q_1, \Delta_{1,1})$; $\sigma(q_2, \sum_{12}) = (q_2, \Delta_{2,2})$; $\sigma(q_3, \sum_{12}) = (q_3, \Delta_{3,3})$; $\sigma(q_4, \sum_{12}) = (q_4, \Delta_{4,4})$; $\sigma(q_6, \sum_{12}) = (q_5, \Delta_{6,5})$; $\sigma(q_8, \sum_{12}) = (q_7, \Delta_{8,7})$
Chip conveying (off → on)	$s_{i4} = 0$ and $s_{j4} = 1$	$\sigma(q_1, \sum_4) = (q_1, \Delta_{1,1})$; $\sigma(q_2, \sum_4) = (q_2, \Delta_{2,2})$; $\sigma(q_3, \sum_4) = (q_3, \Delta_{3,3})$; $\sigma(q_4, \sum_4) = (q_4, \Delta_{4,4})$; $\sigma(q_5, \sum_4) = (q_7, \Delta_{5,7})$; $\sigma(q_6, \sum_4) = (q_8, \Delta_{6,8})$
Chip conveying (on → off)	$s_{i4} = 1$ and $s_{j4} = 0$	$\sigma(q_1, \sum_5) = (q_1, \Delta_{1,1})$; $\sigma(q_2, \sum_5) = (q_2, \Delta_{2,2})$;; $\sigma(q_3, \sum_5) = (q_3, \Delta_{3,3})$; $\sigma(q_4, \sum_5) = (q_4, \Delta_{4,4})$; $\sigma(q_7, \sum_5) = (q_5, \Delta_{7,5})$; $\sigma(q_8, \sum_5) = (q_6, \Delta_{8,6})$
Spindle rotating (Ls → Hs)	$s_{i5} = 0$ and $s_{j5} = 1$; $s_{i5} = 1$ and $s_{j5} = 1((n_j > n_i))$	$\sigma(q_1, \sum_8) = (q_2, \Delta_{1,2})$; $\sigma(q_2, \sum_8) = (q_2, \Delta_{2,2})$;; $\sigma(q_3, \sum_{8,-}) = (q_2, \Delta_{3,2})$; $\sigma(q_4, \sum_{8,-}) = (q_2, \Delta_{4,2})$; $\sigma(q_9, \sum_{8,-}) = (q_2, \Delta_{9,2})$; $\sigma(q_{10}, \sum_{8,-}) = (q_2, \Delta_{10,2})$
Spindle rotating (Hs → Ls)	$s_{i5} = 1$ and $s_{j5} = 0$; $s_{i5} = 1$ and $s_{j5} = 1((n_j \leq n_i))$	$\sigma(q_2, \sum_9) = (q_1, \Delta_{2,1})$; $\sigma(q_2, \sum_8) = (q_2, \Delta_{2,2})$; $\sigma(q_3, \sum_9) = (q_1, \Delta_{3,1})$; $\sigma(q_4, \sum_8) = (q_2, \Delta_{4,2})$; $\sigma(q_9, \sum_8) = (q_2, \Delta_{9,2})$; $\sigma(q_{10}, \sum_8) = (q_2, \Delta_{10,2})$
Positioning (Ls → Hs)	$s_{i6} = 0$ and $s_{j6} = 1$; $s_{i7} = 0$ and $s_{j7} = 1$; $s_{i8} = 0$ and $s_{j8} = 1$	$\sigma(q_2, \sum_6) = (q_3, \Delta_{2,3})$; $\sigma(q_3, \sum_6) = (q_3, \Delta_{3,3})$; $\sigma(q_4, \sum_6) = (q_3, \Delta_{4,3})$; $\sigma(q_5, \sum_6) = (q_3, \Delta_{5,3})$; $\sigma(q_9, \sum_6) = (q_3, \Delta_{9,3})$; $\sigma(q_{10}, \sum_6) = (q_3, \Delta_{10,3})$
Positioning (Hs → Ls)	$s_{i6} = 1$ and $s_{j6} = 0$; $s_{i7} = 1$ and $s_{j7} = 0$; $s_{i8} = 1$ and $s_{j8} = 0$	$\sigma(q_3, \sum_7) = (q_4, \Delta_{3,4})$; $\sigma(q_{3,-}) = (q_2, \Delta_{3,2})$; $\sigma(q_{3,-}) = (q_1, \Delta_{3,1})$
Tool changing (off → on)	$s_{i9} = 0$ and $s_{j9} = 1$; $s_{i10} = 0$ and $s_{j10} = 1$	$\sigma(q_1, \sum_{10}) = (q_9, \Delta_{1,9})$; $\sigma(q_1, \sum_{10}) = (q_{10}, \Delta_{1,10})$;; $\sigma(q_2, \sum_{10}) = (q_9, \Delta_{2,9})$; $\sigma(q_2, \sum_{10}) = (q_{10}, \Delta_{2,10})$; $\sigma(q_3, \sum_{10}) = (q_9, \Delta_{3,9})$; $\sigma(q_3, \sum_{10}) = (q_{10}, \Delta_{3,10})$
Tool changing (on → off)	$s_{i9} = 1$ and $s_{j9} = 0$; $s_{i10} = 1$ and $s_{j10} = 0$	$\sigma(q_{9,-}) = (q_1, \Delta_{9,1})$;; $\sigma(q_{10,-}) = (q_1, \Delta_{10,1})$
Material cutting (off → on)	$s_{i11} = 0$ and $s_{j11} = 1$	$\sigma(q_{4,-}) = (q_5, \Delta_{4,5})$
Material cutting (on → off)	$s_{i11} = 1$ and $s_{j11} = 0$	$\sigma(q_{5,-}) = (q_4, \Delta_{5,4})$; $\sigma(q_{6,-}) = (q_4, \Delta_{6,4})$; $\sigma(q_{7,-}) = (q_4, \Delta_{7,4})$; $\sigma(q_{8,-}) = (q_4, \Delta_{8,4})$

State set: q_0 = machine off; q_1 = standby; q_2 = spindle idling; q_3 = rapid position; q_4 = feed; q_5 = cut; q_6 = cut and cutting fliud spray; q_7 = cut and; chip convery; q_8 = cut and chip convery and cutting fliud spray; q_9 = tool select; q_{10} = tool change. Event set: $\sum_0$ = start machine-M_{start}; $\sum_1$ = close machine-M_{close};$\sum_2$ = open lighting-L_{open}; $\sum_3$ = off lighting-L_{off}; $\sum_4$ = open chip conveyor-M74; $\sum_5$ = off chip conveyor-M75; $\sum_6$ = position-G00; $\sum_7$ = feed-G01/02/03; $\sum_8$ = speedup spindle-M03/04; $\sum_9$ = stop spindle-M05; $\sum_{10}$ = change cutter-M06/64/65; $\sum_{11}$ = open cooling-M07/08; $\sum_{12}$ = off cooling-M09

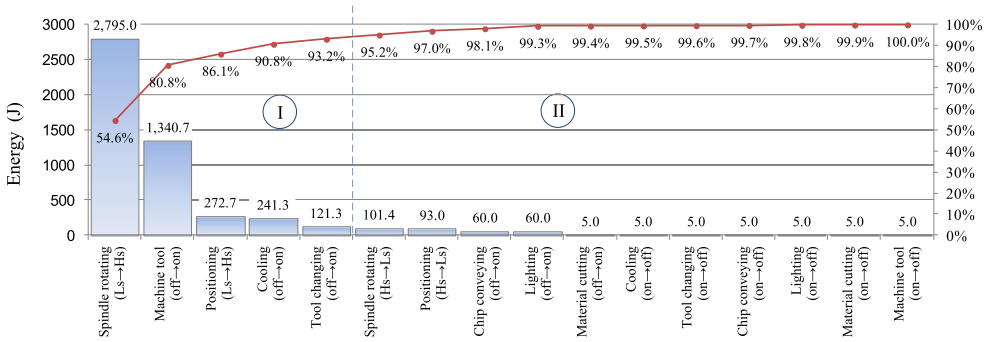

Fig. 6 Pareto chart of energy consumption of transient state

and the energy consumption of machine tool (off → on) is the sum of energy consumption caused by three sub-motions. Considering that the duration of transient state "machine tool (off → on)" varies with different operators, accurate energy consumption of machine tool (off → on) is difficult to be calculated. Therefore, the energy consumption of machine tool (off → on) is not considered in the scope of this paper. Consequently, transient states "spindle rotating (Ls → Hs)," "positioning (Ls → Hs)," "cooling (off → on)," and "tool changing (off → on)" are selected as key transient states (category I) and other transient states are classified as non-critical transient states (category II). According to the Pareto chart, energy consumption of key transient states accounted for over 80 % of the total energy consumption of transient states.

3.2 Energy consumption models of key transient states

3.2.1 Energy consumption model of spindle rotating (Ls → Hs)

Spindle rotating (Ls → Hs) is the transient state of the spindle accelerating from low speed to high speed without cutting loading. Power curve of an actual transient state "spindle rotating (Ls → Hs)" of CK6153*i* CNC lathe is shown in Fig. 7 (initial spindle speed is n_1 and target spindle speed is n_2). Energy consumption of transient state "spindle rotating (Ls → Hs)" (E_{SRA}) is calculated as:

$$E_{SRA} = E_{SR1} + E_{SR2} + E_{SR3} \tag{2}$$

where E_{SR1} is the energy consumption of a spindle system from spindle rotating start to peak power, J; E_{SR2} is the energy consumption of a spindle system from peak power to spindle rotating finish, J; E_{SR3} is energy consumption of supporting therblig during transition state, J.

E_{SR1} can further be calculated as [14, 20]:

$$E_{SR1} = \int_0^{t_{SR1}} P_{SR1}dt = \int_0^{t_{SR1}} [P_{SR}(n_1 + 30\alpha t/\pi) + T_s(\pi n_1/30 + \alpha t)]dt \tag{3}$$

where P_{SR1} is the power of spindle system from spindle rotating start to peak power, W; $P_{SR}()$ is power function spindle system; n_1 is initial spindle speed, r/min; α is angular acceleration of spindle, rad/s^2; T_s is equivalent acceleration torque of spindle system, N · m; t_{SR1} is duration from spindle rotating start to peak power, s; T_s and α can be obtained through spindle startup experiment [46].

The energy consumption of spindle system from peak power to stable power is written as:

$$E_{SR2} = 0.5[P_{SR\max} + P_{SR}(n_2)]t_{SR2} \tag{4}$$

where $P_{SR\max}$ is power peak of spindle speedup, W; $P_{SR}()$ is the spindle power function, W; n_2 is target spindle speed, r/min; t_{SR2} is the duration from peak power to spindle rotating finish, s.

$P_{SR\max}$ is spindle accelerating power at the moment t_{SR1}. Based on Eq. (3), $P_{SR\max}$ can also be expressed as

$$P_{SR\max} = P_{SR1}(t_{SR1}) = P_{SR}\left(n_1 + 30\alpha t_{SR1}\Big/\pi\right) + T_s\left(\pi n_1\Big/30 + \alpha t_{SR1}\right) \tag{5}$$

E_{SR3} is relevant to the status of supporting therbligs during transient state. The statuses of supporting therbligs are judged according to the state vector of forward machining state [20]. The value 1 (except the current changing therblig) in state vector of forward machining state reflected as the supporting therblig. For instance, machining state q_1 standby changes to state q_2 spindle idling, and the corresponding state vector changes from $\vec{MS}_1$= [1, 1, 0, 0, 0, 0, 0, 0, 0, 0, 0] to $\vec{MS}_2$= [1, 1, 0, 0, 1, 0, 0, 0, 0, 0, 0]. The logistic representation of executing state of therblig-spindle rotating in state vector is changing from 0 to 1. Hence, the first (standby operating) and second (lighting) therbligs are identified as supporting therbligs. Moreover, if the spindle accelerating from low speed to high speed and the corresponding state vector changes from $\vec{MS}_1$= [1, 1, 0, 0, 1, 0, 0, 0, 0, 0, 0] to $\vec{MS}_2$= [1, 1, 0, 0, 1, 0, 0, 0, 0, 0, 0], then the state vector of

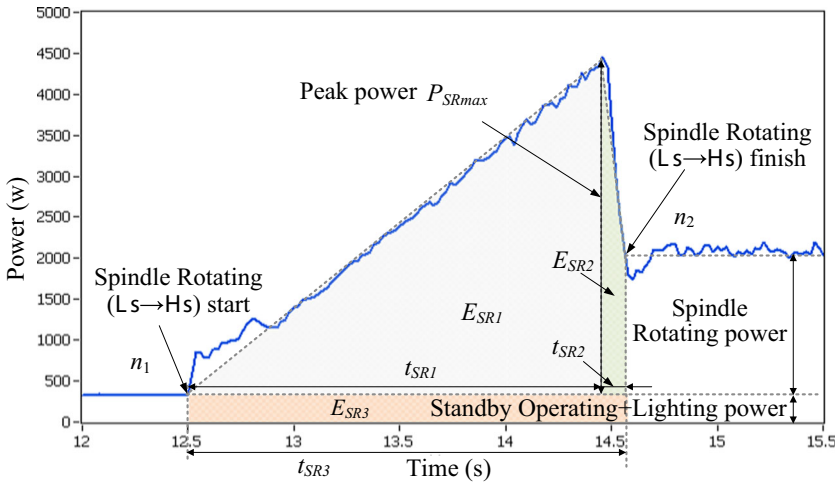

Fig. 7 Power curve of spindle rotating (Ls → Hs)

forward machining state during this transient state is $\vec{MS}_1 = [1, 1, 0, 0, 1, 0, 0, 0, 0, 0, 0]$. Because the fifth therblig is the current changing therblig, the supporting therbligs are also first (standby operating) and second (lighting) therblig. E_{SR3} is calculated as

$$E_{SR3} = \int_0^{t_{SR3}} \vec{MP} \times \vec{MS}\ dt \tag{6}$$

where $\vec{MP}$ is the power vector of forward machining state; $\vec{MS}$ is the state vector of forward machining state; t_{SR3} is the duration of transient state ($t_{SR3} = t_{SR1} + t_{SR2}$), s. Among them, $\vec{MP} = (P_{SO}, P_L, \cdots, P_{MC})$; $\vec{MS} = (s_1, s_2, \cdots, s_{11})^T$.

The energy consumption of supporting therblig during state transition process is further calculated as

$$E_{SR3} = \int_0^{t_{SR3}} \begin{bmatrix} P_{SO}\cdot s_1 + P_L\cdot s_2 + P_{CFS}\cdot s_3 + P_{CC}\cdot s_4 \\ + P_{SR}\cdot s_5 + P_{XF}\cdot s_6 + P_{YF}\cdot s_7 \\ + P_{ZF}\cdot s_8 + P_{TS}\cdot s_9 + P_{TC}\cdot s_{10} + P_{MC}\cdot s_{11} \end{bmatrix} dt \tag{7}$$

where P_{SO} is power of therblig-standby operating, W; P_L is power of therblig-lighting, W; P_{CFS} is of power of therblig-cutting fluid spraying; P_{CC} is of power of therblig-chip

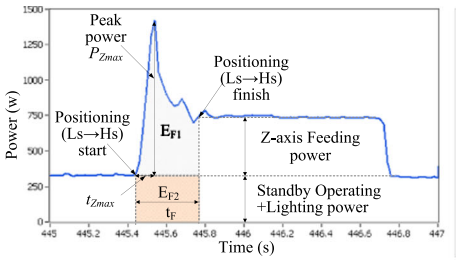

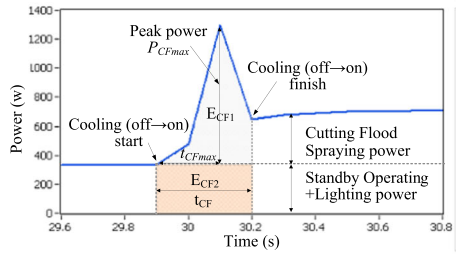

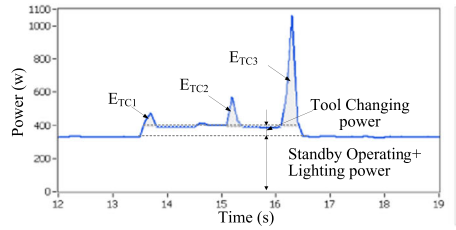

Fig. 8 Energy consumption models of positioning (Ls → Hs)/ cooling (off → on)/tool changing (off → on)

(a) Energy consumption model of positioning(Ls→Hs)

$$E_{FA} = E_{F1} + E_{F2} = \int_0^{t_F} P_{F1}(t)\,dt + \int_0^{t_F} \begin{bmatrix} P_{SO}\cdot s_1 + P_L\cdot s_2 + P_{CFS}\cdot s_3 + P_{CC}\cdot s_4 \\ + P_{SR}\cdot s_5 + P_{XF}\cdot s_6 + P_{YF}\cdot s_7 + P_{ZF}\cdot s_8 \\ + P_{TS}\cdot s_9 + P_{TC}\cdot s_{10} + P_{MC}\cdot s_{11} \end{bmatrix} dt$$

Where, E_{FA} is energy consumption of positioning (Ls→Hs), J; E_{F1} is energy consumption of feeding system during positioning (Ls→Hs), J; E_{F2} is energy consumption of supporting therblig during positioning (Ls→Hs), J; t_F is duration of positioning (Ls→Hs),s; $P_{F1}(t)$ is power function of feeding system.

(b) Energy consumption model of cooling(off→on)

$$E_{CFA} = E_{CF1} + E_{CF2} = E_{CF1} + \int_0^{t_{CF}} \begin{bmatrix} P_{SO}\cdot s_1 + P_L\cdot s_2 + P_{CFS}\cdot s_3 + P_{CC}\cdot s_4 \\ + P_{SR}\cdot s_5 + P_{XF}\cdot s_6 + P_{YF}\cdot s_7 + P_{ZF}\cdot s_8 \\ + P_{TS}\cdot s_9 + P_{TC}\cdot s_{10} + P_{MC}\cdot s_{11} \end{bmatrix} dt$$

Where, E_{CFA} is energy consumption of cooling(off→on), J; E_{CF1} is energy consumption of cooling device during cooling (off→on), J; E_{CF2} is energy consumption of supporting therblig during cooling (off→on), J; t_{CF} is duration of cooling (off→on),s.

(c) Energy consumption model of tool changing(off→on)

$$E_{TCA} = \sum_{k=1}^{K_{\Delta p}} E_{TC_{\Delta pk}} \qquad \Delta p = \begin{cases} T_{pt} - T_{pi}, & T_{pt} \geq T_{pi} \\ T_p - |T_{pt} - T_{pi}|, & T_{pt} < T_{pi} \end{cases}$$

Where, E_{TCA} is energy consumption of tool changing(off→on), J; $E_{TC\Delta pk}$ is energy consumption of power peak caused by sub-action k when rotating position number of turret is Δp, J; $K_{\Delta p}$ is the number of power peak when rotating position number of turret is Δp; T_{pi} is the initial position of the turret; T_{pt} is the target position of the turret; T_p is the total posts of the turret.

conveying, W; P_{SR} is of power of therblig-spindle rotating, W; P_{XF} is of power of therblig-X-axis feeding, W; P_{YF} is of power of therblig-Y-axis feeding, W; P_{ZF} is of power of therblig-Z-axis feeding, W; P_{TS} is of power of therblig-tool selecting, W; P_{TC} is of power of therblig-tool changing, W; P_{MC} is power of therblig-material cutting, W; $s_1 \sim s_{11}$ are logical representations of therblig-standby operating, lighting, cutting fluid spraying, chip conveying, spindle rotating, X-axis feeding, Y-axis feeding, Z-axis feeding, tool selecting, tool changing, and material cutting, respectively.

t_{SR1} is calculated as

$$t_{SR1} = 2\pi(n_2 - n_1)/60\alpha \tag{8}$$

According to the previous experimental results [20], t_{SR2} is related to target spindle speed n_2 and can be expressed as the liner function of n_2

$$t_{SR2} = A_{SR2} + B_{SR2} \cdot n_2 \tag{9}$$

where A_{SR2} and B_{SR2} are fitting coefficients.

3.2.2 Energy consumption models of positioning (Ls → Hs), cooling (off → on), and tool changing (off → on)

Similarly, energy consumption models of positioning (Ls → Hs), cooling (off → on), and tool changing (off → on) are also developed according to their respective energy consumption characteristics. The energy consumption models of positioning (Ls → Hs), cooling (off → on), and tool changing (off → on) are shown in Fig. 8. For the specific derivation processes of energy consumption models, you can refer to reference [20].

Table 2 Mapping relationship between activities and events

Activity	Event
Operating standby	$\sum_0$ = start machine-M_{start}
Closing machine	$\sum_1$ = close machine-M_{close}
Turning on lighting	$\sum_2$ = open lighting-L_{open}
Turning off lighting	$\sum_3$ = off lighting-L_{off}
Turning on conveyor	$\sum_4$ = open chip conveyor-M74
Turning off conveyor	$\sum_5$ = off chip conveyor-M75
Rapid positioning-x(y/z)	$\sum_6$ = position-G00
Feeding/cutting-x(y/z)	$\sum_7$ = feed-G01/02/03
Rotating spindle	$\sum_8$ = speedup spindle-M03/04
Stop spindle	$\sum_9$ = stop spindle-M05
Selecting/changing cutter	$\sum_{10}$ = change cutter-M06/64/65
Turning on cooling device	$\sum_{11}$ = open cooling-M07/08
Turning off cooling device	$\sum_{12}$ = off cooling-M09

Table 3 Relationship among activity-machining state event

Activity	Machining state	Event
–	$q_{\tau 1}$ (initial state)	–
A_1	$q_{\tau 2}$	$\sum_{k1}$
A_2	$q_{\tau 3}$	$\sum_{k2}$
A_3	$q_{\tau 2}$	$\sum_{k3}$
A_4	$q_{\tau 4}$	$\sum_{k4}$
A_5	$q_{\tau 4}$	$\sum_{k5}$
A_6	$q_{\tau 2}$	$\sum_{k6}$
A_7	$q_{\tau 1}$	$\sum_{k7}$

3.3 Energy consumption computation of transient states of machining process

3.3.1 Establishing state transition chart

According to the mapping relationship between activity and machining state [20], the corresponding machining states of activities are determined. Starting time of activity corresponds to an event; the event is used to trigger a state transition. The mapping relationship between activity and event is shown in Table 2.

Supposing seven activities (A_1~A_7) are decomposed from machining process, corresponding machining states of the above seven activities are obtained (shown in Table 3) based on the mapping relationship between activities and machining states. And the corresponding events of seven activities are also determined (last column in Table 3) according to the mapping relationship between activities and events (Table 2).

The initial state of the above machining process is $q_{\tau 1}$, and activity A_1 corresponds to the event $\sum_{k1}$. According to the sequence of the machining state, the first state transition can be determined $\sigma(q_{\tau 1}, \sum_{k1}) = (q_{\tau 2}, \Delta_{\tau 1,\tau 2})$. In state transition chart, the arc without a source state points to the initial state $q_{\tau 1}$. Input event $\sum_{k1}$ that triggers the transition is labeled on the left of "/," and output information $\Delta_{\tau 1,\tau 2}$ of state transition is labeled on the right of "/." $\Delta_{\tau 1,\tau 2}$ includes two parts ${\Delta_{\tau 1,\tau 2}}^E$ and ${\Delta_{\tau 1,\tau 2}}^t$. ${\Delta_{\tau 1,\tau 2}}^E$ represents energy consumption of transition from state $q_{\tau 1}$ to state $q_{\tau 2}$. ${\Delta_{\tau 1,\tau 2}}^t$ represents duration of transition from state $q_{\tau 1}$ to state $q_{\tau 2}$.On the basis of state transition chart that only contains the first state transition $\sigma(q_{\tau 1},$

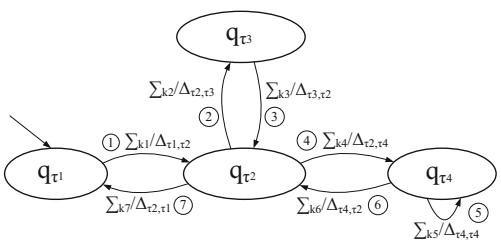

Fig. 9 State transition chart

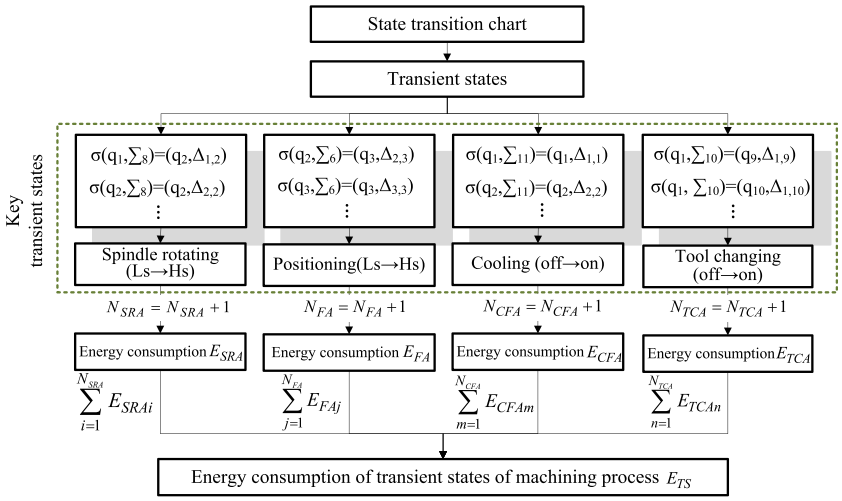

Fig. 10 Calculation process of energy consumption of transient states of machining process

$\sum_{k1}) = (q_{\tau 2}, \Delta_{\tau 1,\tau 2})$, continue to build state transition chart using state $q_{\tau 2}$ as input of the second state transition. According to Table 3, the event that triggers the second state transition is $\sum_{k2}$, and state tansfers from $q_{\tau 2}$ to $q_{\tau 3}$. Therefore, the second state transition is $\sigma(q_{\tau 2}, \sum_{k2}) = (q_{\tau 3}, \Delta_{\tau 2,\tau 3})$. Similarly, the input event $\sum_{k2}$ and output information $\Delta_{\tau 2,\tau 3}$ are labeled on both sides of "/" between states $q_{\tau 2}$ and $q_{\tau 3}$. Followed by analogy, a complete state transition chart of the above machining process can be established, as shown in Fig. 9.

3.3.2 Energy consumption computing of transient states

According to the established state transition chart of machining process, the key transient states and corresponding executing times are obtained by combining classification of transient states (Table 1). The calculation process of energy consumption of transient states of machining process is shown in Fig. 10.

(1) N_{SRA}, N_{FA}, N_{CFA}, and N_{TCA} denote the number of execution of transient state spindle (Ls → Hs), positioning (Ls → Hs), cooling (off → on), and tool changing (off → on), respectively. Initial value are set as $N_{SRA} = 0$, $N_{FA} = 0$, $N_{CFA} = 0$, and $N_{TCA} = 0$.

(2) Actually, all the state transitions of the machining process can be determined according to the established state transition chart $\sigma(q_i, \sum_k) = (q_j, \Delta_{i,j})$. The transient state type can be judged based on the classification table of transient state (Table 1) then the key transient states (spindle(Ls → Hs), positioning(Ls → Hs), cooling (off → on), and tool changing (off → on) can be figure out.

(3) When the transient state is spindle (Ls → Hs), $N_{SRA} = N_{SRA} + 1$ is executed; when the transient state is positioning (Ls → Hs) then judge the relationship between feed distance L_f and critical feed distance L_{f0},, when $L_f \geq L_{f0}$, $N_{FA} = N_{FA} + 1$ is executed; when the transient state is cooling (off → on), $N_{CFA} = N_{CFA} + 1$ is executed; when the transient state is tool changing (off → on), $N_{TCA} = N_{TCA} + 1$ is executed.

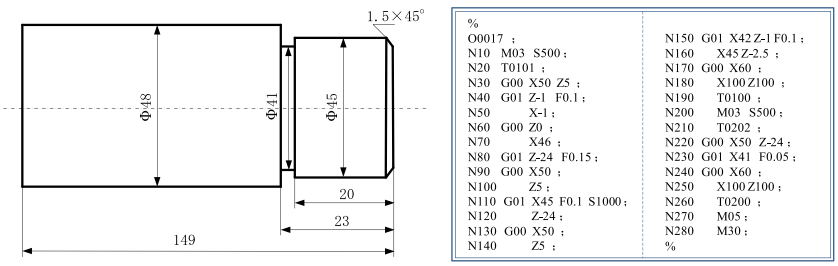

	Spindle speed n (r/min)	Feedrate f (mm/r)	Depth of cutting a_p (mm)	Length of cutting l (mm)	Cutter
① Face turning	500	0.10	1.00	24.00	1#
② Rough external turning	500	0.15	1.00	23.00	1#
③ Fine external turning	1000	0.10	0.50	23.00	1#
④ Chamfering	1000	0.10	1.50	1.50	1#
⑤ Grooving	500	0.05	2.00	3.00	2#

Fig. 11 Example workpiece, NC program, and main cutting parameters

(4) After the execution of $N_{SRA}=N_{SRA}+1$, energy consumption of transient state spindle (Ls → Hs) E_{SRA} is calculated based on the developed energy consumption model of spindle rotating (Ls → Hs) in Section 3.2. Similarly, after the execution of $N_{FA}=N_{FA}+1$, $N_{CFA}=N_{CFA}+1$, and $N_{TCA}=N_{TCA}+1$, energy consumptions of transient states positioning (Ls → Hs), cooling (off → on), and tool changing (off → on) can be calculated based on the corresponding developed energy consumption models in Section 3.2.

(5) When all are judged completely, the execution times of four types of key transient states (N_{SRA}, N_{FA}, N_{CFA}, and N_{TCA}) have been calculated. Energy consumption of key transient states are accumulated based on the execution time of each type of transient state, and then, energy consumptions of each type of key transient state of the whole machining process can be obtained: $\sum_{i=1}^{N_{SRA}} E_{SRAi}$, $\sum_{j=1}^{N_{FA}} E_{FAj}$, $\sum_{m=1}^{N_{CFA}} E_{CFAm}$, $\sum_{n=1}^{N_{TCA}} E_{TCAn}$.

(6) Energy consumption of transient states of machining process can be obtained by summing up the energy of four types of key transient states $E_{TS}=\sum_{i=1}^{N_{SRA}} E_{SRAi}+\sum_{j=1}^{N_{FA}} E_{FAj}+\sum_{m=1}^{N_{CFA}} E_{CFAm}+\sum_{n=1}^{N_{TCA}} E_{TCAn}$.

4 Case study

To demonstrate the feasibility of the proposed approach, an actual machining case is conducted and analyzed in this case study. An example workpiece was machined through five main cutting processes (1. Face turning, 2. Rough external turning, 3. Fine external turning, 4. Chamfering, 5. Grooving). The diameter and length of the blank are 48 and 150 mm, and the material of the blank is carbon steel (C45). The shape of an example workpiece and corresponding NC program are shown in Fig. 11. The machining processes were carried out on a CK6153*i* CNC lathe, whose X-axis and Z-axis rapid-moving speeds are 6 and 10 m/min, respectively [47]. The main machining parameters are also listed in the bottom of Fig. 11. Number 1 cutting tool is VNMG160408MV (cemented carbide), and number 2 cutting tool is a 3-mm grooving cutter (cemented carbide).

(1) According to the activity extraction method proposed in literature [45], the machining process of example workpiece can be decomposed into 35 activities. Combining with the mapping relationship between activities and running states [20], the activities and corresponding machining states during machining process of example workpiece can be obtained (see Table 4).

(2) The events occur at the starting time of above 35 activities are determined according to the mapping relationship table between activities and events (Table 2), as shown in the last column of Table 4.

(3) Based on the obtained machining states, state sequence, and trigger events, combining with the construction methods of state transition chart in Section 3.3.1, the

Table 4 Corresponding machining state and event of each machining activity of example workpiece

No.	Activity	Machining state	Event
–	–	q_0 (initial state)	–
1	Executing standby	q_1	$\sum_0$
2	Rotating spindle	q_2	$\sum_8$
3	Selecting cutter	q_{10}	$\sum_{10}$
4	Rapid positioning-xz	q_3	$\sum_6$
5	Rapid positioning-z	q_3	–
6	Feeding-z	q_4	$\sum_7$
7	Feeding-x	q_4	$\sum_7$
8	Cutting-x	q_5	–
9	Rapid positioning-z	q_3	$\sum_6$
10	Rapid positioning-x	q_3	$\sum_6$
11	Feeding-z	q_4	$\sum_7$
12	Cutting-z	q_5	–
13	Rapid positioning-x	q_3	$\sum_6$
14	Rapid positioning-z	q_3	$\sum_6$
15	Rotating spindle	q_2	$\sum_8$
16	Feeding-x	q_4	$\sum_7$
17	Feeding-z	q_4	$\sum_7$
18	Cutting-z	q_5	–
19	Rapid positioning-x	q_3	$\sum_6$
20	Rapid positioning-z	q_3	$\sum_6$
21	Feeding-xz	q_4	$\sum_7$
22	Cutting-xz	q_5	$\sum_7$
23	Rapid positioning-x	q_3	$\sum_6$
24	Rapid positioning-xz	q_3	$\sum_6$
25	Rapid positioning-z	q_3	–
26	Rotating spindle	q_2	$\sum_8$
27	Changing cutter	q_{10}	$\sum_{10}$
28	Rapid positioning-xz	q_3	$\sum_6$
29	Rapid positioning-z	q_3	–
30	Feeding-x	q_4	$\sum_7$
31	Cutting-x	q_5	–
32	Rapid positioning-x	q_3	$\sum_6$
33	Rapid positioning-xz	q_3	$\sum_6$
34	Rapid positioning-z	q_3	–
35	Stop spindle	q_1	$\sum_9$

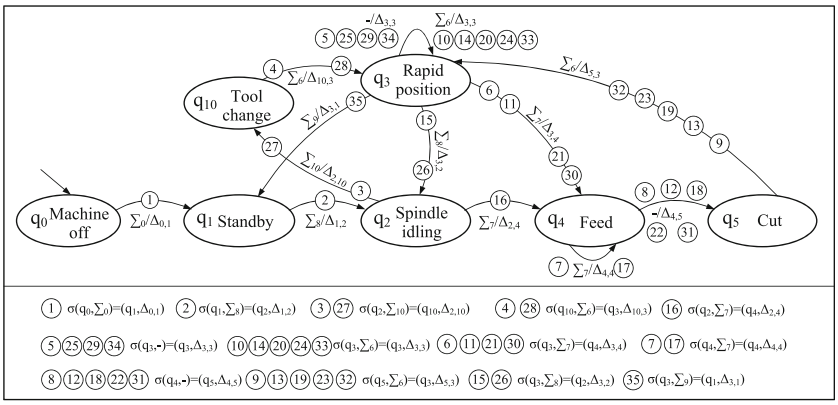

Fig. 12 State transition chart of machining process of example workpiece

state transition chart of machining process of the example workpiece can be developed, as shown in Fig. 12. According to the state transition chart, 35 transient states are obtained.

(4) The derived 35 transient states are distinguished one by one to determine the key transient states and corresponding execution times. The first transient state is $\sigma(q_0, \sum_0)=(q_1, \Delta_{0,1})$, according to the classification table of transient states (Table 1), the transient state type can be determined as machine (off → on). The second transient state is $\sigma(q_1, \sum_8)=(q_2, \Delta_{1,2})$, the transient state type can be determined as key transient state spindle (Ls → Hs) according to Table 1 then $N_{SRA}=N_{SRA}+1$ is executed (initial value of N_{SRA} is 0) and the value of N_{SRA} is updated to 1. When all the above 35 transient states are judged completely, the number of execution times of four types of key transient states can be obtained: $N_{SRA}=2$, $N_{FA}=7$, $N_{CFA}=0$, and $N_{TCA}=2$.

(5) Energy consumption of single key transient states can be calculated by using the established energy consumption model of key transient states in Section 3.2. Taking the 15 transient states as an example, the initial spindle speed is 500 r/min, the target spindle speed is 1000 r/min. For the AH transmission chain of CK61563i CNC lathe, the coefficients T_s and α in formula are $T_s=28.42$ N•m, $\alpha=39.78$ rad/s^2 [14]. According to formula (8), t_{SR1} can be calculated as $t_{SR1}=0.002632(1000-500)=1.32$ s. According to the reference [20], when the spindle speed is less than 1000 r/min, spindle power can be expressed as $P_{SR}=1.09n+41.12$. Then, based on Eq. (3), E_{SR1} can be calculated as $E_{SR1}=\int_0^{1.32}[1.09\times(500+380t)+41.12+2.98\times500+$

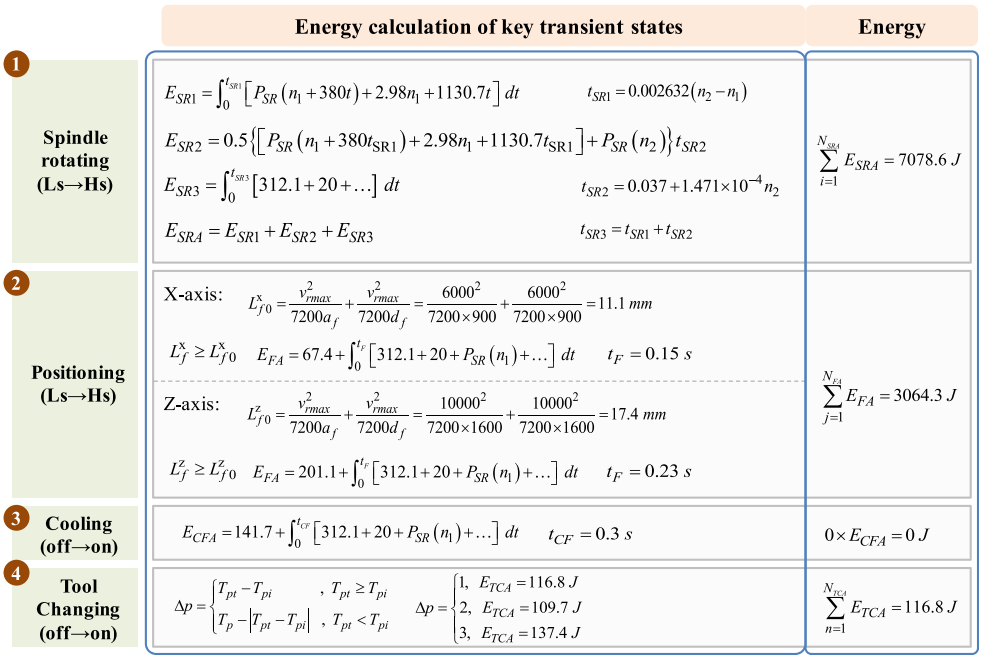

Fig. 13 Energy calculation of transient states of example workpiece

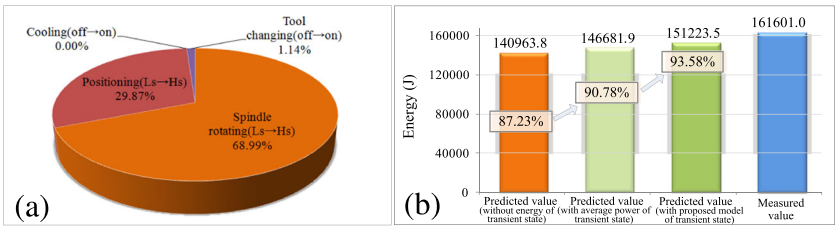

Fig. 14 Energy consumption distribution of transient states and comparison of predicted and measured energy (CK6153*i*)

1130.7*t*]dt = 4086.4 J. According to formula (4), the energy consumption of spindle system from peak power to stable power is calculated as $E_{SR2} = 0.5 \times [P_{SR\max} + P_{SR}(1000)]t_{SR2}$. Based on formula (9) and preliminary experimental data of CK61563i CNC lathe [40], values of coefficients A_{SR2} and B_{SR2} can be obtained, $A_{SR2} = 0.037$ $B_{SR2} = 1.471 \times 10^{-4}$. Then, t_{SR2} can be calculated $t_{SR2} = 0.037 + 1.471 \times 10^{-4} \times 1000 = 0.18$ s. According to formula (5), $P_{SR\max}$ is expressed as $P_{SR\max} = P_{SR1}(1.32)$. Further combining with formulas (3), $P_{SR\max}$ is calculated as $P_{SR\max} = P_{SR1}(1.32) = 1.09 \times (500 + 380 \times 1.32) + 41.12 + 2.98 \times 500 + 1130.7 \times 1.32 = 4115.4$ W. According to the spindle power model $P_{SR} = 1.09n + 41.12$, spindle power can be obtained $P_{SR}(1000) = 1.09 \times 1000 + 41.12 = 1131.1$ W. Hence, E_{SR2} is computed as $E_{SR2} = 0.5 \times (4115.4 + 1131.1) \times 0.18 = 472.2$ J. The state vector of forward machining state during the above transient state is [1, 1, 0, 0, 1, 0, 0, 0, 0, 0, 0], the fifth therblig (spindle rotating) is the current changing therblig, then supporting therbligs are identified as therblig-standby operation ⟨S⟩ and therblig-lighting ⊗. According to the ex ante experimental measurement conducted on CK6153*i*, power values of therblig-standby operation and therblig-lighting of CK6153*i* lathe are $P_{SO} = 312.1$ w and $P_L = 20$ w. The duration of transient state is calculated as $t_{SR3} = t_{SR1} + t_{SR2} = 1.32 + 0.18 = 1.5$ s. Therefore, the energy consumption of supporting therbligs during transition is $E_{SR3} = \int_0^{1.5}(312.1 + 20)dt = 498.2$ J. Then, total energy consumption of transient state spindle (Ls → Hs) is $E_{SRA} = 4086.4 + 472.2 + 498.2 = 5056.8$ J. Similarly, the energy consumption of four types of transient states can be calculated, as shown in Fig. 13.

(6) Based on the calculated energy consumptions of the above four types of key transient states and the derived values $N_{SRA} = 2$, $N_{FA} = 7$, $N_{CFA} = 0$, $N_{TCA} = 2$, total energy consumption of transient states of machining process can be obtained: $E_{AT} = \sum_{i=1}^{2} E_{SRA} + \sum_{j=1}^{7} E_{FA} + \sum_{m=1}^{0} E_{CFA} + \sum_{n=1}^{2} E_{TCA} =$ 10259.7 J.

Figure 14a shows the energy consumption distribution of transient states, it can be seen that energy consumption of transient state spindle (Ls → Hs) is greatest, accounting for 68.99 % of the total energy consumption of the transient states. The reason is that the chuck weight of the spindle system of CNC lathe is large, and the required energy to overcome the inertia of the spindle system is very large. Meanwhile, the acceleration duration from low speed to high speed is also very significant ((some acceleration duration is more than 1.5 s). The second large energy consumption is caused by transient state positioning (Ls → Hs). Although duration of single positioning (Ls → Hs) process is short, the transfer process involves instant increment of momentums of machine table, causing large power peak. Moreover, the positioning (Ls → Hs) frequently occurs during entire machining process. Hence, the energy consumption of positioning (Ls → Hs) is significant, accounting for 29.87 % of the total energy consumption of transient states. Because only two times of tool changing (off → on) during machining process of example workpiece, and the duration of tool changing (off → on) is short, so the energy consumption of tool changing (off → on) is only accounted for 1.14 % of total transient energy consumption. The coolant was not used during machining process of example workpiece; thus, the proportion of cooling (off → on) accounted is 0 %.

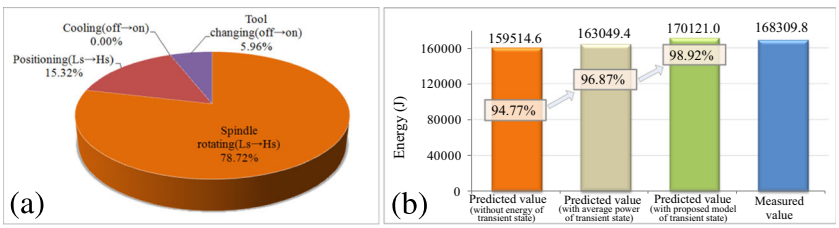

Fig. 15 Energy consumption distribution of transient states and comparison of predicted and measured energy (CAK6150D*i*)

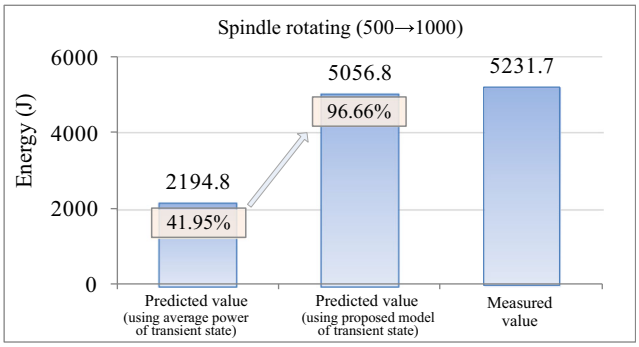

Fig. 16 Comparison of predicted and measured energy for spindle rotating (500 → 1000) (CK6153*i*)

As shown in Fig. 14b, the prediction accuracy of energy consumption of machining process is 87.23 % without considering the energy consumptions of transient states. The accuracy can be achieved 90.78 % by using the average power of the transient state. Moreover, the calculated energy consumption of machining process is 151223.5 J (the measured value is 161601.0 J) when using the proposed energy models of transient states. Then, the prediction accuracy can further be raised from 90.78 to 93.58 %.

The same machining process of the above case (using the same NC program, cutting parameters, blank dimension, materials, and cutters) was repeated on CAK6150D*i* CNC lathe. The main cutting parameters are shown in Fig. 11. The rapid-moving speeds of X-axis and Z-axis of CAK6150D*i* CNC lathe are 5 and 10 m/min, respectively. The rated power of spindle motor is 7.5 kW. The calculated results are shown in Fig. 15. In this machining case, the energy predictive accuracy increases from 94.77 to 96.87 % by using the average power of transient state. With the proposed model in this paper, the predictive accuracy can further be improved from 96.87 to 98.92 %.

It can be seen that predictive accuracy can be improved around 2 % by using the average operation power of the machine for the transient state compared to the energy predicted without energy of transient state. Then, the improvement accuracy from the proposed model would be 2~3 % compared to predictive model with average power of transient state. Obviously, the predictive accuracy can be improved to some extent by using average power of transient state when compared to the situation without considering energy of transient state. However, the accuracy of predictive model with average power of transient state is relatively lower than the model proposed in this paper for single transient state.

Taking transient state spindle rotating (Ls → Hs) as an example, the initial spindle speed is 500 r/min, the target spindle speed is 1000 r/min. (1) Calculating energy with the proposed

Fig. 17 Predicted and measured power curve of machining case (CK6153*i*)

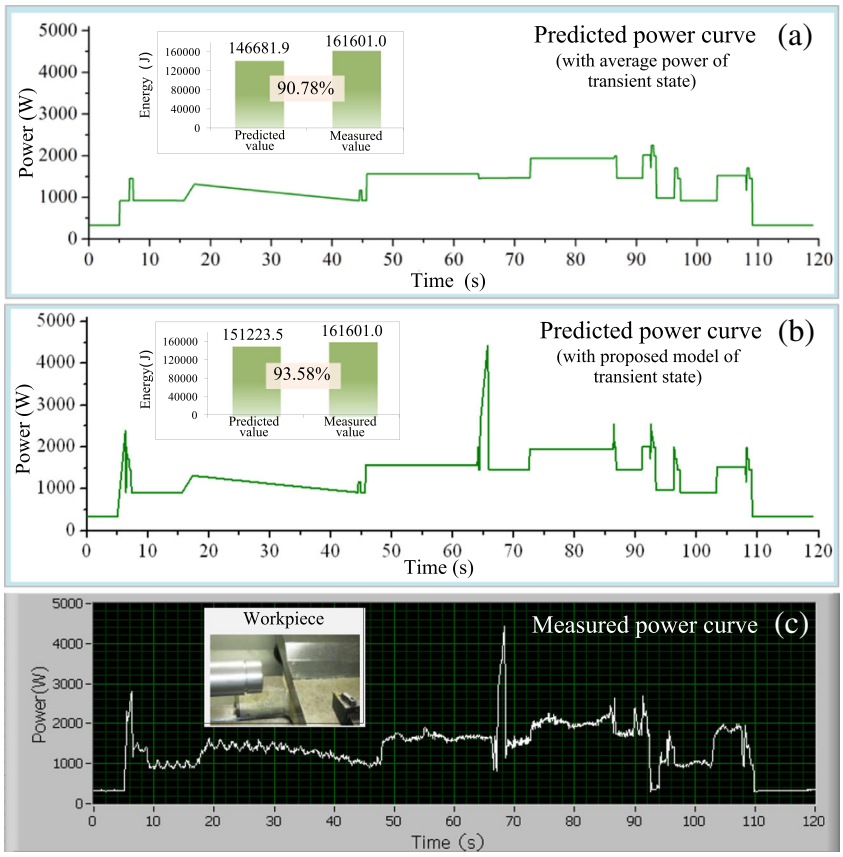

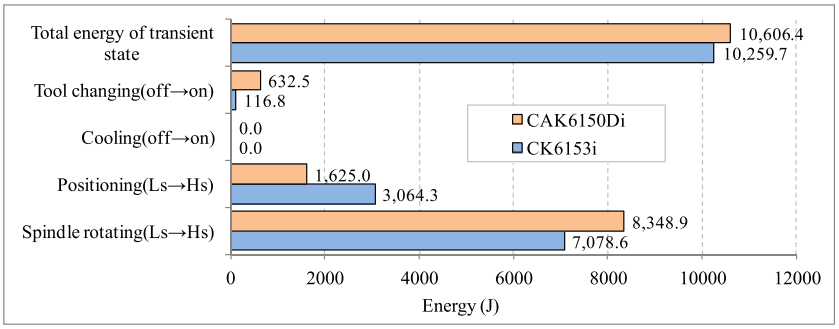

Fig. 18 Comparison of transient state energy consumption between CK6153*i* and CAK6150D*i*

model of transient state in this manuscript: according to the aforementioned computing process, total energy consumption of spindle rotating (500 → 1000) is $E_{SRA} = 4086.4 + 472.2 + 498.2 = 5056.8$ J. (2) Calculating energy with average power of transient state: during the transient state spindle rotating (500 → 1000), the average power of the machine is used and the average power of the machine is composed of spindle rotating power at 1000 r/min, power of standby operation, and lighting of CK6153*i* lathe. According to the spindle power model $P_{SR} = 1.09n + 41.12$, spindle power can be obtained $P_{SR}(1000) = 1.09 \times 1000 + 41.12 = 1131.1$ W. According to the ex ante experimental measurement conducted on CK6153*i*, power values of standby operation and lighting of CK6153*i* lathe are $P_{SO} = 312.1$ W and $P_L = 20$ W. Therefore, the average power of the machine can be calculated $P_{avg} = 1131.1 + 312.1 + 20 = 1463.2$ W. The duration of spindle rotating (500 → 1000) is calculated using the approach in our manuscript $t = 1.32 + 0.18 = 1.5$ s. Hence, total energy consumption of transient state spindle rotating (500 → 1000) is $E_{SRA} = 1463.2 \times 1.5 = 2194.8$ J.

Comparison of predicted and measured energy for spindle rotating (500 → 1000) is shown in Fig. 16. It can be seen that the proposed model in this paper can significantly improve the accuracy compared to the predictive model with average power of transient state. With the increase of the number of transient states (e.g., spindle rotating (Ls → Hs)), the predictive accuracy difference between the two methods will become increasingly large and the advantage of the proposed method in this manuscript will be more and more obvious.

Moreover, Fig. 17 shows the predicted and measured power curve of machining case. It can be seen that the predictive power curve with the proposed model can display the power peaks during machining case. The predicted power curve with the proposed model can match the measured power curve better than the predicted power curve with average power of transient state. The proposed approach can improve the integrity of energy consumption models of the entire machining process and improve the forecasting accuracy of energy consumption of the entire machining process.

Figure 18 shows the comparison of transient state energy consumption between CK6153*i* and CAK6150D*i* when conducting the same machining process. The results show that energy consumption of spindle rotating (Ls → Hs) is the largest of four types of transient states, and transient state positioning (Ls → Hs) consumed more energy on CAK6150D*i*. The reason is that peak power of transient state has positive correlation with T_s (equivalent acceleration torque of spindle) and α (angular acceleration of spindle) (according to Eq. 5). The values of T_s and α of CAK6150D*i* lathe are both larger than that of CK6153*i*, as shown in Fig. 19.Under the same machining conditions, the peak power of CAK6150D*i* lathe is larger than that of CK6153i. The larger power peak makes energy consumption of spindle rotating (Ls → Hs) on CAK6150D*i* is relatively greater. Furthermore, the energy consumption proportion of spindle rotating (Ls → Hs) is the largest of four types of transient states (accounted for more than 65 %) then it makes entire energy consumption of transient states of CAK6150Di greater than CK6153i for the given

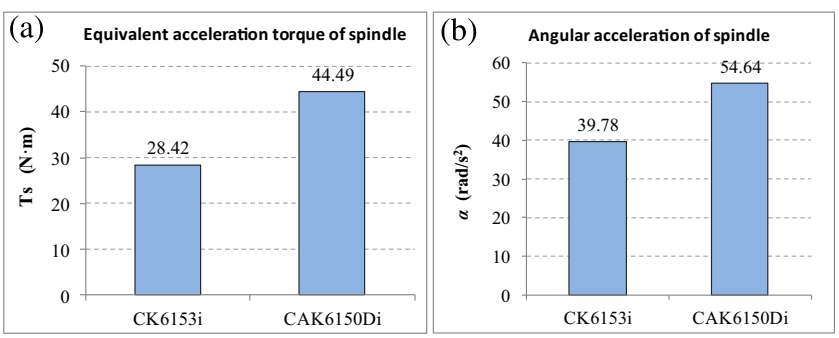

Fig. 19 Comparison of T_s and α between CK6153*i* and CAK6150D*i*

machining case. Thus, energy consumption of transient states can be reduced by selecting the CK6153*i* CNC lathe to execute the machining process of the given case.

5 Conclusions

Energy consumption modeling of machining processes is the foundation of energy optimization, and energy consumption of machining transient states is an important part. Considering energy consumption characteristics of transient states, FSM is introduced into the energy consumption modeling of machining transient states in this paper. Firstly, transient states during machining process are described by the FSM model, and then, classification of transient states is conducted. Four types of key transient states are identified, including spindle rotating (Ls → Hs), positioning (Ls → Hs), cooling (off → on), and tool changing (off → on). The energy consumption model of the above four types of key transient states are established. The state transition chart of machining process is developed, and each transient state is evaluated to figure out the key transient states and corresponding execution times. Then, the energy consumption of transient states of entire machining process can be computed combining the established energy consumption model of four types of key transient states. Finally, taking the machining process of a common stepped shaft part as an example, case studies of the proposed method are conducted. The results showed that the development of energy consumption of transient states can improve the energy prediction accuracy of the entire machining process (increasing 6.35 and 4.15 % in two machining cases compared to predictive model without energy of transient state; the improvement accuracies are 2.80 and 2.05 % in two machining cases when compared to the predictive model with average power of transient state). The proposed method can also improve the integrity of energy consumption model of machining processes and provide more accurate energy model for machining energy optimization.

The energy consumption of machining processes includes energy consumption of steady states and transient states. The energy consumption modeling of transient states is focused on this paper, and a complete energy consumption model of machining process can be established combined with the previous established energy model of steady states. Further research will be conducted on energy optimization issue considering both energy consumptions of steady states and transient states.

Acknowledgments The authors sincerely thank all the anonymous reviewers for their valuable suggestions on the improvement of our paper. This research is supported by the National Natural Science Foundation, China (No.51175464); the National High Technology Research and Development Program of China (863 program, No. 2013BAF02B10); and the Scientific Research Foundation of Shandong University of Science and Technology for Recruited Talents (No. 2015RCJJ049).

References

1. Duflou JR, Sutherland JW, Dornfeld D, Herrmann C, Jeswiet J, Kara S, Hauschild M, Kellens K (2012) Towards energy and resource efficient manufacturing: a processes and systems approach. CIRP Ann Manuf Technol 61(2):587–609
2. Liu Y, Dong H, Lohse N, Petrovic S, Gindy N (2014) An investigation into minimising total energy consumption and total weighted tardiness in job shops. J Clean Prod 65:87–96
3. International Energy Agency (IEA) (2007) Tracking industrial energy efficiency and CO2 emission. OECD/IEA, Paris
4. Tang D, Du K, Li L (2006) On the development path of Chinese manufacturing industry based on resource restraint. Jiangsu Soc Sci 4:51–58
5. Shao G, Kibira D, Lyons K (2010) A virtual machining model for sustainability analysis. In: Proceedings of the ASME 2010 international design engineering technical conferences & computers and information in engineering conference. Montreal, Quebec. pp.1-9
6. Gutowski T (2011) Energy and environmental issues for manufacturing processes. http://web.mit.edu/2.810/www/lecture2011/Environment.pdf. (Accessed 26 Jan 2013)
7. Zulaika JJ, Dietmair A, Campa FJ, López de Lacalle LN, Verbeeten W (2010) Eco-efficient and highly productive production machines by means of a holistic eco-design approach, The 3rd International Conference on Eco-Efficiency Modelling and Evaluation for Sustainablity: Guiding Eco-Innovation and Consumption, Egmond an Zee, The Netherlands
8. Gutowski T, Dahmus J, Thiriez A (2006) Electrical energy requirements for manufacturing processes. In: Proceedings of 13th CIRP International Conference on Life Cycle Engineering, Leuven. pp. 623-628
9. Wang Q, Liu F, Wang X (2013) Multi-objective optimization of machining parameters considering energy consumption. Int J Adv Manuf Technol 71:1133–1142
10. Balogun VA, Mativenga PT (2013) Modeling of direct energy requirements in mechanical machining processes. J Clean Prod 41: 179–186
11. Li J-g, Lu Y, Zhao H, Li P, Yao Y-x (2013) Optimization of cutting parameters for energy saving. Int J Adv Manuf Technol 70:117–124
12. Peng T, Xu X (2014) Energy-efficient machining systems: a critical review. Int J Adv Manuf Technol 72(9-12):1389–1406
13. Velchev S, Kolev I, Ivanov K, Gechevski S (2014) Empirical models for specific energy consumption and optimization of cutting parameters for minimizing energy consumption during turning. J Clean Prod 80:139–149
14. Lv JX, Tang RZ, Jia S (2014) Therblig-based energy supply modeling of CNC machine tools. J Clean Prod 65:168–177
15. Yoon HS, Lee JY, Kim MS, Ahn SH (2014) Empirical power-consumption model for material removal in three-axis milling. J Clean Prod 78:54–62
16. Jia S, Tang R, Lv J, Zhang Z, Yuan Q (2015) Energy modeling for variable material removal rate machining process: an end face turning case. Int J Adv Manuf Technol. doi:10.1007/s00170-015-8133-8
17. Tristo G, Bissacco G, Lebar A, Valentinčič J (2015) Real time power consumption monitoring for energy efficiency analysis in micro EDM milling. Int J Adv Manuf Technol 78:1511–1521
18. Zhong Q, Tang R, Lv J, Jia S, Jin M (2015) Evaluation on models of calculating energy consumption in metal cutting processes: a case of external turning process. Int J Adv Manuf Technol. doi:10.1007/s00170-015-7477-4
19. Liu F, Xie J, Liu S (2015) A method for predicting the energy consumption of the main driving system of a machine tool in a machining process. J Clean Prod 105:171–177

20. Jia S (2014) Research on energy demand modeling and intelligent computing of machining process for low carbon manufacturing. Zhejiang University, Hangzhou
21. Santos JP, Oliveira M, Almeida FG, Pereira JP, Reis A (2011) Improving the environmental performance of machine-tools: influence of technology and throughput on the electrical energy consumption of a press-brake. J Clean Prod 19(4):356–364
22. Campatelli G, Lorenzini L, Scippa A (2014) Optimization of process parameters using a response surface method for minimizing power consumption in the milling of carbon steel. J Clean Prod 66: 309–316
23. O'Driscoll E, Kelly K, O'Donnell GE (2015) Intelligent energy based status identification as a platform for improvement of machine tool efficiency and effectiveness. J Clean Prod 105:184–195
24. Yi Q, Li C, Tang Y, Chen X (2015) Multi-objective parameter optimization of CNC machining for low carbon manufacturing. J Clean Prod 95:256–264
25. Zhang Y (2014) Energy efficiency techniques in machining process: a review. Int J Adv Manuf Technol 71:1123–1132
26. Ma J, Ge X, Chang SI, Lei S (2014) Assessment of cutting energy consumption and energy efficiency in machining of 4140 steel. Int J Adv Manuf Technol 74:1701–1708
27. Xie J, Liu F, Qiu H (2015) An integrated model for predicting the specific energy consumption of manufacturing processes. Int J Adv Manuf Technol. doi:10.1007/s00170-015-8033-y
28. Herrmann C, Thiede S (2009) Process chain simulation to foster energy efficiency in manufacturing. CIRP J Manuf Sci Tech 1(4): 221–229
29. Li W, Kara S (2011) An empirical model for predicting energy consumption of manufacturing processes: a case of turning process. Proc Inst Mech Eng B J Eng Manuf 225(9):1636–1646
30. Yan J, Li L (2013) Multi-objective optimization of milling parameters—the trade-offs between energy, production rate and cutting quality. J Clean Prod 52:462–471
31. Balogun VA, Edem IF, Mativenga PT (2015) The effect of auxiliary units on the power consumption of CNC machine tools at zero load cutting. Int J Sci Eng Res 6(2):874–879
32. Balogun VA, Edem IF, Mativenga PT (2016) E-smart toolpath machining strategy for process planning. Int J Adv Manuf Technol. doi:10.1007/s00170-015-8286-5
33. Abele E, Sielaff T, Schiffler A, Rothenbücher S (2011) Analyzing energy consumption of machine tool spindle units and identification of potential for improvements of efficiency. In: Proceedings of the 18th CIRP International Conference on Life Cycle Engineering, Braunschweig. pp.281-285
34. Lee J-Y, Shin Y-J, Kim M-S, Kim E-S, Yoon H-S, Kim S-Y, Yoon Y-C, Ahn S-H, Min S (2015) A simplified machine-tool power-consumption measurement procedure and methodology for estimating total energy consumption. J Manuf Sci Eng 138(051004):1–9
35. Huang J, Liu F, Xie J (2015) A method for determining the energy consumption of machine tools in the spindle start-up process before machining. Proc Inst Mech Eng B J Eng Manuf. doi:10.1177/0954405415600679
36. He Y, Liu F, Wu T, Zhong FP, Peng B (2011) Analysis and estimation of energy consumption for numerical control machining. Proc Inst Mech Eng B J Eng Manuf 226(2):255–266
37. Reinhart G, Reinhardt S, Föckerer T, Zäh MF (2011) Comparison of the resource efficiency of alternative process chains for surface hardening. In: Proceedings of 18th CIRP International Conference on LCE, Braunschweig. pp 311-316
38. Avram OI, Xirouchakis P (2011) Evaluating the use phase energy requirements of a machine tool system. J Clean Prod 19(6-7):699–711
39. Shi J, Liu F, Xu D, Chen GR (2009) Decision model and practical method of energy-saving in NC machine tool. China Mech Eng 20(11):1344–1346
40. Lv JX (2014) Research on energy supply modeling of computer numerical control machine tools for low carbon manufacturing. Zhejiang University, Hangzhou
41. Harel MD (1987) Statecharts: a visual formalism for complex systems. Sci Comput Program 8:231–274
42. Girault A, Lee B, Lee EA (1999) Hierarchical finite state machines with multiple concurrency models. Proc IEEE Trans Comput Aided Des Integr Circuits Syst 18(6):742–760
43. Li X, Wang Y, Liang H, Zhong L (2005) Finite state machine application in open CNC. Comput Integr Manuf Syst 11(3):428–432
44. Jia S, Tang RZ, Lv JX (2014) Therblig-based energy memand modeling methodology of machining process to support intelligent manufacturing. J Intell Manuf 25(5):913–931
45. Jia S, Tang RZ, Lv JX (2014) Machining activity extraction and energy attributes inheritance method to support intelligent energy estimation of machining process. J Intell Manuf. doi:10.1007/s10845-014-0894-7
46. Tang RZ, Lv JX, Jia S (2014) A method for acquiring the spindle speedup power and energy of CNC machine tool and corresponding energy-saving approach. Patent CN201410095872.0, China
47. CK6153i series (2000) Manual specification of CK6153i series CNC lathe. Jinan First Machine Tool Group Co., Ltd. of China